Pairing correlations and resonant states in the relativistic mean field theory

N. Sandulescu,[1,2,3] L. S. Geng,[3,4] H. Toki,[3] and G. C. Hillhouse[3,5]
[1]*Royal Institute of Technology, SCFAB, SE-10691 Stockholm, Sweden*
[2]*Institute for Physics and Nuclear Engineering, P.O. Box MG-6, 76900 Bucharest, Romania*
[3]*Research Center for Nuclear Physics (RCNP), Osaka University, 10-1 Mihogaoka, Ibaraki, Osaka 567-0047, Japan*
[4]*School of Physics, Peking University, Beijing 100871, People's Republic of China*
[5]*Department of Physics, University of Stellenbosch, Matieland 7602, South Africa*
(Received 5 June 2003; published 25 November 2003)

We present a simple scheme for taking into account the resonant continuum coupling in the relativistic mean field-BCS calculations. In this scheme, applied before in nonrelativistic calculations, the effect of the resonant continuum on pairing correlations is introduced through the scattering wave functions located in the region of the resonant states. These states are found by solving the relativistic mean field equations with scattering-type boundary conditions for the continuum spectrum. The calculations are done for the neutron-rich Zr isotopes. It is shown that the sudden increase of the neutron radii close to the neutron drip line, the so-called giant halo, is determined by a few resonant states close to the continuum threshold.

DOI: 10.1103/PhysRevC.68.054323 PACS number(s): 21.60.Jz, 21.10.Gv, 27.60+j

I. INTRODUCTION

As recognized a long time ago [1], the basic features of superfluidity are the same in atomic nuclei and infinite Fermi systems. Yet, in atomic nuclei the pairing correlations have many features related to the finite size of the system. The way in which the finite size affects the pairing correlations depends on the position of the chemical potential. If the chemical potential is deeply bound, such as in stable and heavy nuclei, the finite size influences the pairing correlations mainly through the shell structure induced by the spin-orbit interaction. The situation becomes more complex in nuclei close to the drip lines, where the chemical potential approaches the continuum threshold. In this case the inhomogeneity of the pairing field produces strong mixing between the bound and the continuum parts of the single-particle spectrum. Due to this mixing the quasiparticle spectrum becomes dominated by resonant quasiparticle states, which originate both from single-particle resonances and deep hole states [2–5].

The continuum effects on pairing correlations is commonly taken into account in the Hartree-Fock-Bogoliubov (HFB) [6] or relativistic-Hartree-Bogoliubov (RHB) [7] approach. In most of these calculations the continuum is replaced by a set of positive energy states determined by solving the HFB or RHB equations in coordinate space and with box boundary conditions [8,9]. Due to this fact the genuine continuum properties, as the widths of the quasiparticle resonant states, are not accounted for straightforwardly in these types of calculations.

Recently the HFB equations were also solved with exact boundary conditions for the continuum spectrum, both for a zero range [5] and a finite range pairing forces [10]. It was thus shown that close to the drip lines the discretization of the continuum generally overestimates the pairing correlations. A similar conclusion was obtained earlier in a simpler BCS approach, in which the resonant part of the continuum was studied [11,12]. Comparing these BCS results with the exact HFB solutions [5] one finds that for the heavy nuclei close to the drip line the main effect of the continuum on pairing correlations is given usually by a few resonant states close to the continuum threshold.

For the relativistic models an exact solution of the continuum spectrum is not available yet, neither for RHB nor for relativistic mean field-BCS (RMF-BCS) approach. A comparison between RHB and RMF-BCS calculations, performed by using box boundary conditions, is discussed in Ref. [13]. This comparison indicates also the special role played by the resonant states, which in these calculations are approximated by positive energy states. This approximation works well only if the positive energy states correspond to very narrow resonances. Moreover, since a discrete representation of the continuum does not provide a direct measure of the width of the resonant states, the selection of the relevant positive energy states is ambiguous if the resonant states close to the continuum threshold are not very narrow.

The scope of this paper is to show how the resonant continuum can be treated accurately in the RMF-BCS approach. The single-particle states belonging to the resonant part of the continuum spectrum will be calculated by solving the RMF equations with scattering-type boundary conditions. Then the resonant continuum will be handled in the BCS equations in a similar way as in the nonrelativistic HF-BCS calculations [12]. This approach is applied for the case of Zr isotopes for which earlier calculations predict a very large neutron skin close to the neutron drip line. It is shown that the sudden increase of the nuclear radii in these isotopes is essentially determined by a few single-particle resonant states close to the continuum threshold.

The article is organized as follows. In Sec. II we discuss shortly the scattering-type solutions of the relativistic mean field equations and we introduce the resonant-BCS equations [12]. Then in Sec. III we present the results of the calculations for Zr isotopes. Sec. IV contains the summary of the paper.

II. RESONANT STATES IN THE RMF-BCS APPROACH

A. Continuum-RMF solutions

In the relativistic mean field approach the nuclear interaction is usually described by the exchange of three mesons: the scalar meson σ, which mediates the medium-range attraction between the nucleons, the vector meson ω, which mediates the short-range repulsion, and the isovector-vector meson $\vec{\rho}$, which provides the isospin dependence of the nuclear force. The equations of motion are commonly derived from the effective Lagrangian density [7,14]

$$\begin{aligned}\mathcal{L} = &\bar{\psi}[\imath\gamma^{\mu}\partial_{\mu} - M]\psi + \frac{1}{2}\partial_{\mu}\sigma\partial^{\mu}\sigma - \frac{1}{2}m_{\sigma}^{2}\sigma^{2} - \frac{1}{3}g_{2}\sigma^{3} - \frac{1}{4}g_{3}\sigma^{4} \\ &- g_{\sigma}\bar{\psi}\sigma\psi - \frac{1}{4}H_{\mu\nu}H^{\mu\nu} + \frac{1}{2}m_{\omega}^{2}\omega_{\mu}\omega^{\mu} + \frac{1}{4}c_{3}(\omega_{\mu}\omega^{\mu})^{2} \\ &- g_{\omega}\bar{\psi}\gamma^{\mu}\psi\omega_{\mu} - \frac{1}{4}G_{\mu\nu}^{a}G^{a\mu\nu} + \frac{1}{2}m_{\rho}^{2}\rho_{\mu}^{a}\rho^{a\mu} - g_{\rho}\bar{\psi}\gamma_{\mu}\tau^{a}\psi\rho^{\mu a} \\ &- \frac{1}{4}F_{\mu\nu}F^{\mu\nu} - e\bar{\psi}\gamma_{\mu}\frac{(1-\tau_{3})}{2}A^{\mu}\psi, \end{aligned} \tag{1}$$

where a nonlinear self-coupling is considered both for σ and ω mesons. The vector fields H, G, and F are given by

$$H_{\mu\nu} = \partial_{\mu}\omega_{\nu} - \partial_{\nu}\omega_{\mu},$$

$$G_{\mu\nu}^{a} = \partial_{\mu}\,\rho_{\nu}^{a} - \partial_{\nu}\,\rho_{\mu}^{a} - 2g_{\rho}\epsilon^{abc}\,\rho_{\mu}^{b}\rho_{\nu}^{c},$$

$$F_{\mu\nu} = \partial_{\mu}A_{\nu} - \partial_{\nu}A_{\mu}.$$

The nucleons are described by the Dirac spinor field ψ, which in the case of spherical symmetry can be written as

$$\psi = \frac{1}{r}\begin{pmatrix} i & G & \mathcal{Y}_{jlm} \\ F & \sigma\cdot & \hat{r}\mathcal{Y}_{jlm}\end{pmatrix}, \tag{2}$$

where $\mathcal{Y}_{jlm}$ denotes the spinor spherical harmonics, while G and F are the radial wave functions for the upper and lower components, respectively. They satisfy the radial equations

$$\frac{dG}{dr} + \frac{\kappa}{r}G - (M + E + V_{s} - V_{v})F = 0, \tag{3}$$

$$-\frac{dF}{dr} + \frac{\kappa}{r}F + (M - E + V_{s} + V_{v})G = 0, \tag{4}$$

where V_s and V_v are the scalar and the vector mean fields and κ is given by

$$\kappa = \begin{cases} -(l+1) & \text{if} \quad j = l + 1/2 \\ +l & \text{if} \quad j = l - 1/2. \end{cases} \tag{5}$$

At large distances, where both the scalar and the vector mean fields are zero, the radial equations can be written in the form

$$\frac{d^{2}G}{dr^{2}} + \left(\alpha^{2} - \frac{\kappa(\kappa+1)}{r^{2}}\right)G = 0, \tag{6}$$

$$F = \frac{1}{E+M}\left(\frac{dG}{dr} + \frac{\kappa}{r}G\right), \tag{7}$$

where $\alpha^2 = E^2 - M^2$. These equations are suited for fixing the scattering-type boundary conditions for the continuum spectrum. They are given by

$$G = C\alpha r[\cos(\delta)j_{l}(\alpha r) - \sin(\delta)n_{l}(\alpha r)], \tag{8}$$

$$F = \frac{C\alpha^{2}r}{E+M}[\cos(\delta)j_{l-1}(\alpha r) - \sin(\delta)n_{l-1}(\alpha r)], \tag{9}$$

where j_l and n_l are the Bessel and Neumann functions and δ is the phase shift associated to the relativistic mean field. The constant C is fixed by the normalization condition of the scattering wave functions and the phase shift δ is calculated from the matching conditions. In the vicinity of an isolated resonance the derivative of the phase shift has a Breit-Wigner form, i.e.,

$$\frac{d\delta(E)}{dE} = \frac{\Gamma/2}{(E_{r} - E)^{2} + \Gamma^{2}/4} \tag{10}$$

from which one estimates the energy and the width of the resonance. In the vicinity of a resonance the radial wave functions of the scattering states have a large localization inside the nucleus. Close to a resonance the energy dependence of both components of the Dirac wave functions can be factorized approximatively by a unique energy dependent function [15]. As in the nonrelativistic case [16], this energy dependent factor is the square root of the Breit-Wigner function written above, or, equivalently, the square root of the derivative of the phase shift. Using this property all the matrix elements of a two-body interaction between these scattering states can be expressed in term of a unique matrix element, i.e., the one corresponding to the scattering state with energy equal to the energy of the resonance. This property is employed below for the treatment of the resonant continuum in the BCS equations.

B. Resonant states in the BCS approach

Since the meson exchange forces do not properly describe the pairing correlations in nuclei, the relativistic mean field is combined usually with nonrelativistic pairing models. Here we use for the pairing treatment the BCS approach and for the pairing force we take a δ-type interaction.

Compared to the approximations based on the general Bogoliubov transformation, e.g., HFB and RHB, in the BCS approach the correlations induced by the pairs formed in states that are not time-reversed partners are neglected. Although these correlations can induce particular effects when the coupling to the continuum states is taken into account, e.g., the widths of deep hole states, their relative contribution to the physical properties of drip line nuclei appears to be of less importance [5,12,13].

In the BCS approach applied here the coupling to the continuum is introduced through the resonant states located nearby the Fermi level. In heavy nuclei close to the drip line, these states have usually the dominant contribution to the pairing correlations [5,11,13]. This is expected since the resonant states, trapped by the centrifugal or Coulomb barrier, are much more localized inside the nucleus compared to the nonresonant continuum states. For the neutron *s*-waves, which are not trapped by a centrifugal barrier, the localization of the scattering wave functions inside the nucleus can be relatively large, and eventually important for pair correlations, only if there is an antibound state close to the continuum threshold [15]. This is a rather special case, known so far only in light halo nuclei, e.g., ^{11}Li [22].

The extension of the BCS equations for taking into account the resonant continuum was proposed in Refs. [11,12]. For the case of a general pairing interaction these equations, referred below as the resonant-BCS (rBCS) equations, reads [12]

$$\Delta_i = \sum_j V_{i\bar{i}j\bar{j}} u_j v_j + \sum_\nu V_{i\bar{i},\nu\epsilon_\nu\overline{\nu\epsilon_\nu}} \int_{I_\nu} g_\nu(\epsilon) u_\nu(\epsilon) v_\nu(\epsilon) d\epsilon, \tag{11}$$

$$\Delta_\nu \equiv \sum_j V_{\nu\epsilon_\nu\overline{\nu\epsilon_\nu}j\bar{j}} u_j v_j + \sum_{\nu'} V_{\nu\epsilon_\nu\overline{\nu\epsilon_\nu},\nu'\epsilon_{\nu'}\overline{\nu'\epsilon_{\nu'}}} \int_{I_{\nu'}} g_{\nu'}(\epsilon') u_{\nu'}(\epsilon') v_{\nu'}(\epsilon') d\epsilon', \tag{12}$$

$$N = \sum_i v_i^2 + \sum_\nu \int_{I_\nu} g_\nu^c(\epsilon) v_\nu^2(\epsilon) d\epsilon. \tag{13}$$

Here Δ_i are the gaps for the bound states and Δ_ν are the averaged gaps for the resonant states. The quantity $g_\nu^c(\epsilon) = (2j_\nu + 1/\pi)(d\delta_\nu/d\epsilon)$ is the total level density and δ_ν is the phase shift of angular momentum $l_\nu j_\nu$. The factor $g_\nu^c(\epsilon)$ takes into account the variation of the localization of scattering states in the energy region of a resonance (i.e., the width effect) and goes to a δ function in the limit of a very narrow width. The interaction matrix elements are calculated with the scattering wave functions at resonance energies and normalized inside the volume where the pairing interaction is active. For more details see Ref. [12].

The rBCS equations written above are applied here with the single-particle spectrum of the RMF equations. For the pairing interaction we use in the following section a δ force, i.e., $V = V_0 \delta(\vec{r}_1 - \vec{r}_2)$. In this case the matrix elements of the pairing interaction are given by

$$\langle (\tau_1\bar{\tau}_1)0^+ | V | (\tau_2\bar{\tau}_2)0^+ \rangle = \frac{V_0}{8\pi} \int dr \frac{1}{r^2} (G^\star_{\tau_1} G_{\tau_2} + F^\star_{\tau_1} F_{\tau_2})^2. \tag{14}$$

For the resonant states these matrix elements are calculated as mentioned above, i.e., using the radial wave functions evaluated at resonance energies and normalized inside a finite volume.

The RMF and the rBCS equations are solved iteratively. At each iteration the densities are modified through the occupation probabilities provided by the rBCS, as in the nonrelativistic HF-rBCS calculations [12].

III. RMF-rBCS CALCULATIONS FOR NEUTRON-RICH Zr ISOTOPES

Zr isotopes were discussed recently in connection to the so-called giant halo structure, which these isotopes may develop close to the neutron drip line [17]. In Ref. [17] these isotopes were calculated by solving the RHB equations in coordinate representation and using box boundary conditions. The mean field was described by using the parameter set NLSH [18] and for the pairing interaction was employed a density dependent δ interaction. In the calculations all the positive energy states up to 120 MeV were considered.

In order to compare our calculations with the RHB predictions of Ref. [17] we use for the mean field the same parameter set, i.e., NLSH. The results are not much different even when we use other parameter sets, e.g., NL3 and TM1 [19,20]. The appropriate choice for the pairing interaction is more difficult because the pairing correlations estimated with a zero range force depend strongly on the energy cutoff, which is very different in the two calculations. Thus in the RMF-rBCS approach we include from all the continuum only a few resonant states close to zero energy, while in the RHB calculations the pairs are virtually scattered in all the positive energy states up to the energy cutoff, i.e., 120 MeV. This energy cutoff here is much larger than the maximum quasiparticle energy calculated in RMF-rBCS, which corresponds to the single-particle bound state $1s_{1/2}$. Due to these facts we cannot compare meaningfully the results of the two calculations if we use the same zero range force. The best we can do is to choose in the RMF-rBCS calculations a pairing force which provides on average pairing energies close to the RHB values, at least for some isotopes. Following this procedure we chose in the RMF-rBCS calculations a zero range pairing force given by $V = V_0(\mathbf{r}_1 - \mathbf{r}_2)$, with $V_0 = -275$ MeV. We found that the strength of the force can be actually increased up to about $V_0 = -350$ MeV without affecting significantly the separation energies and the nuclear radii shown below.

First we analyze the behavior of the single-particle states in the vicinity of the continuum threshold. These states play the major role in the formation of the neutron skin structure discussed below. The neutron single-particle levels for the *Zr* isotopes closest to the neutron drip line, i.e., from the mass number $A = 120$ up to $A = 138$ are shown in Fig. 1. The dashed line represents the chemical potential, which stays close to zero from $A = 124$ to $A = 138$. The positive energies shown here are the energies of the resonant states. As seen in Fig. 1, the states $2f_{5/2}$, $1h_{9/2}$, and $1i_{13/2}$ remain resonant states for all the isotopes, and their energies are changing with the neutron number in the same way as the energy of the bound state $1h_{11/2}$. The other three states, i.e., $2f_{7/2}$, $3p_{3/2}$, and $3p_{1/2}$, are resonant states for $A < 126$ and become loosely bound states

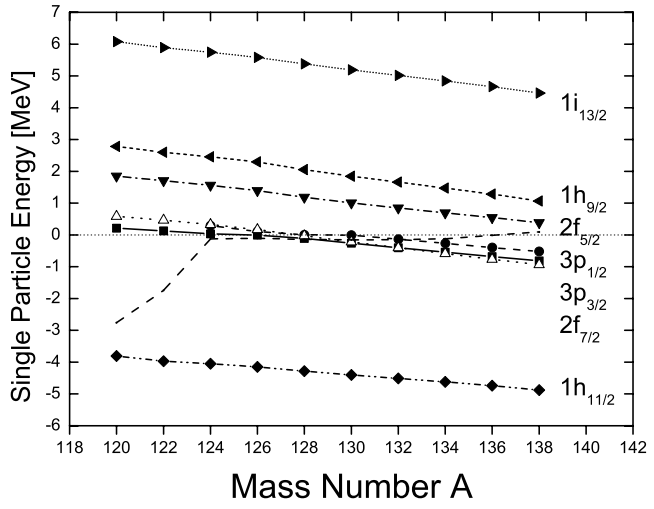

FIG. 1. The energies of bound and resonant single-particle states close to the continuum threshold in Zr isotopes. The Fermi energy is shown by the dashed line.

for heavier isotopes. Their radial wave functions for $A=124$ are shown in Fig. 2. The figure shows the upper components of the radial wave functions calculated at the resonance energies for which their localization inside the nucleus is the largest.

The widths of the resonant states are plotted in Fig. 3. The resonant states $1h_{9/2}$ and $2f_{5/2}$ have rather small widths for all the isotopes. On the other hand the widths of the resonant states $3p_{1/2}$ and $3p_{3/2}$ are changing dramatically with the neutron number. This is especially the case for the resonant state $3p_{1/2}$. Considering that these states with low lj values have a major contribution to the formation of the neutron skin, their wave functions should be calculated accurately, both for positive and negative energies. The resonant states with high lj values give instead the dominant contribution to the pairing correlations. Since these resonant states have a small width they could be eventually treated like quasibound states in the pairing calculations.

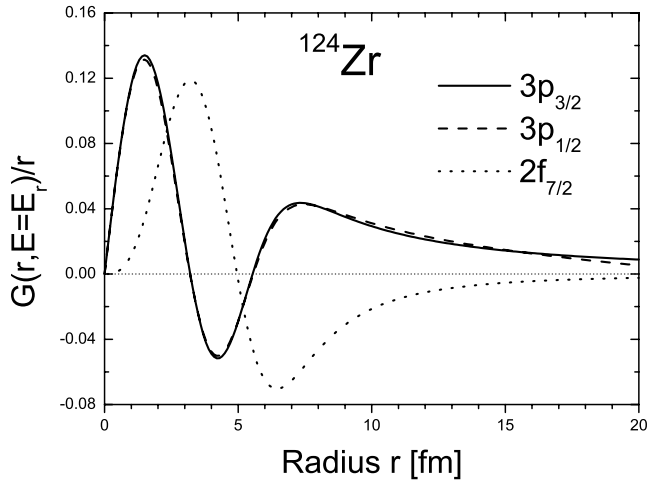

FIG. 2. The radial wave functions of the resonant states $2f_{7/2}$, $3p_{3/2}$, and $3p_{1/2}$ in ^{124}Zr. The plot represents the upper components of the radial wave functions calculated at the resonance energies.

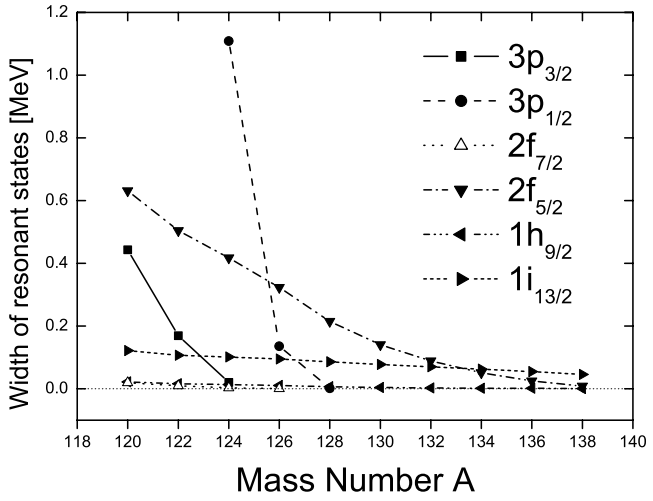

FIG. 3. The width of the single-particle resonant states shown in Fig. 1.

Next we examine the two-neutron separation energies S_{2n}, i.e.,

$$S_{2n}(Z,N) = B(Z,N) - B(Z,N-2). \tag{15}$$

Their values are shown in Fig. 4. The empirical values correspond to Ref. [21] and the RHB results are from Ref. [17].

One can see that RMF-rBCS gives practically the same results as the RHB calculations. The two-neutron separation energies remain close to zero all the way from $A=124$ to $A=138$, which in RMF corresponds to the filling of the group of states $2f_{7/2}$, $3p_{3/2}$, and $3p_{1/2}$.

In order to see the amount of the pairing correlations in these isotopes we plotted in Fig. 5 the pairing correlation energies, i.e., the binding energies referred to the RMF values. The pairing correlation energy curve shows a minimum for $A=136$, which corresponds to the filling of the states

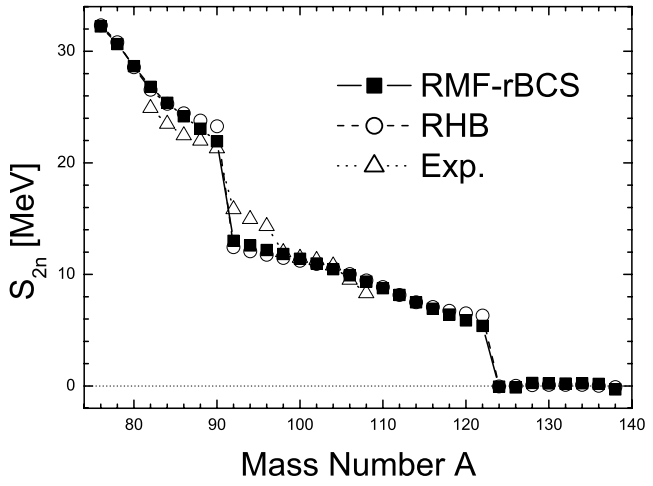

FIG. 4. The two-neutron separation energies of even Zr isotopes as a function of the mass number A.

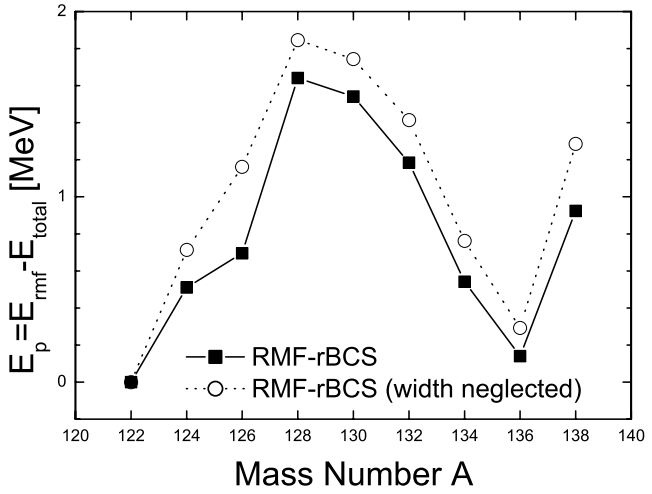

FIG. 5. Pairing correlation energies of even Zr isotopes as a function of the mass number *A*.

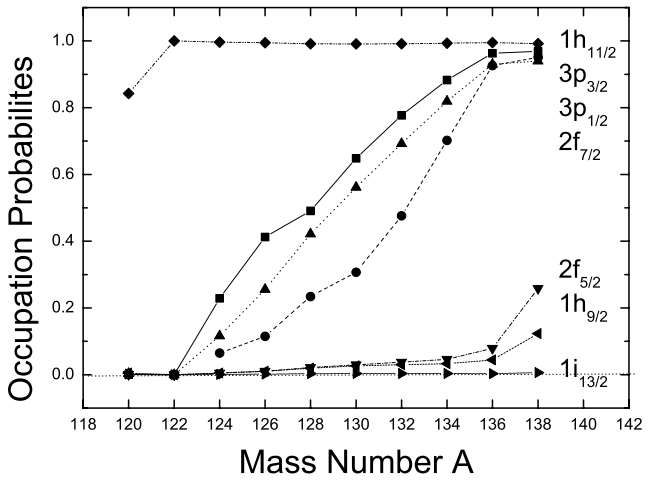

FIG. 7. The occupation probabilities of single-particle states shown in Fig. 1 as a function of the mass number *A*.

$2f_{7/2}$, $3p_{3/2}$. These states have almost the same energy and behave like a closed major shell for the pairing correlation energy.

As discussed in Refs. [5,11], the pairing correlations usually become stronger when the widths of resonant states is not taken into account, i.e., when the resonant states are considered as quasibound state. This effect can also be seen in Fig. 5. On the other hand, the effect of the widths of resonant states is practically negligible for the two-neutron separation energies plotted in Fig. 4. This is because the effect of the widths on pairing energies is washed out by the subtraction performed in Eq. (15). Actually this is also the reason why the two-neutron separation energies are not too much sensitive to the details of the pairing models (e.g., volume or surface pairing).

The most interesting phenomenon in these isotopes is the behavior of the neutron radii, which are shown in Fig. 6. First, one notices that the RMF-rBCS results follow again very closely the RHB values. As shown in Fig. 6, the neutron radii increases sharply from $A=122$ to $A=124$. From the Figs. 7 and 8 one can see that this is mainly due to the filling of the states $3p_{3/2}$, $2f_{7/2}$, and $3p_{1/2}$. For $A=124$ the wide resonant state $3p_{1/2}$ has almost the same energy as the resonant state $3p_{3/2}$, but its relative contribution to the radius is smaller. The states $3p_{3/2}$, $3p_{1/2}$, and $3f_{7/2}$, which give the dominant contribution to the tail of the radii, become quasibound or loosely bound states for $A>126$ and the occupation probabilities of the resonant states $2f_{5/2}$ and $1h_{9/2}$ remain relatively small for all the isotopes. Therefore the calculated radii are practically insensitive to the widths of the resonant states. From Fig. 7 we can see also that the occupancy of the highest resonant state introduced in the calculations, i.e., $1i_{13/2}$, is negligible. Thus for the pairing interaction used in the present RMF-rBCS calculations the energy of the resonant state $1i_{13/2}$ acts like a natural cutoff for the pairing correlations induced by the resonant continuum states.

The behavior of the nuclear radii close to the drip line is very sensitive to the relative occupancy of the loosely bound states and the low-lying narrow resonances with high angular

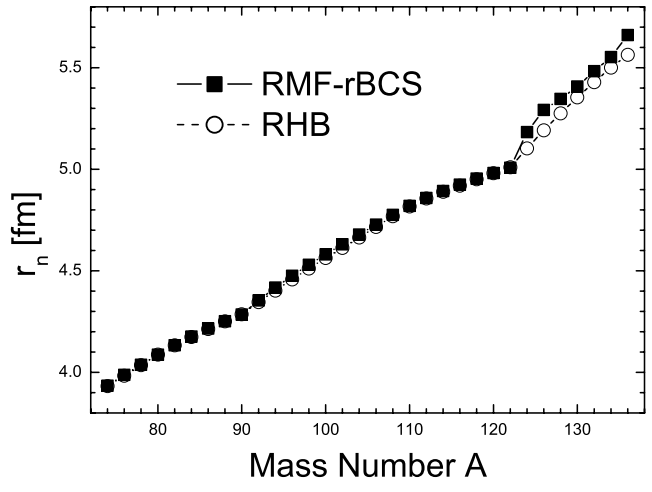

FIG. 6. The root mean square neutron radii of even Zr isotopes as a function of the mass number *A*.

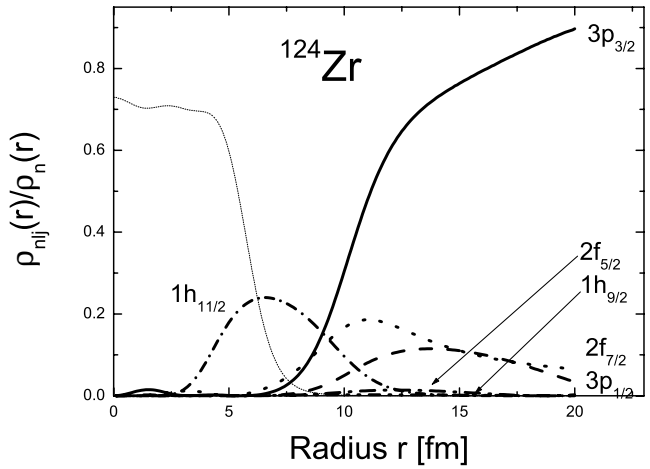

FIG. 8. The relative contribution of single-particle states to the nuclear radius of ^{124}Zr. The dotted line shows the total radius multiplied by a factor of 8.

momenta. Thus if the diffusivity of the Fermi sea is increasing the pairs scatter from the loosely bound states to the narrow resonances, which are more localized around the nucleus. Consequently the nuclear radii might decrease if the average pairing gap is increasing.

This effect can also be seen in the present calculations. In the RHB calculations the occupancy of the narrow resonances with high angular momenta is larger than in RMF-rBCS calculations. Accordingly, as seen in Fig. 6, the RHB radii are smaller than in RMF-BCS calculations. This situation is quite general since in the RHB or HFB calculations, based on a big energy cutoff, the Fermi sea is usually more diffusive than in the rBCS-type calculations, even if the pairing correlation energies might be rather similar in the two calculations. Summarizing this point, the reason why the RMF-rBCS radii in Fig. 6 are larger than the RHB radii is due to the fact that in the RMF-rBCS calculations the occupancy of the loosely bound states are larger and not because there are more particles scattered in the non-localised continuum states.

IV. CONCLUSIONS

In this paper we discussed how the resonant states can be treated accurately in the RMF-BCS approach. The resonant states are described through the scattering states located in the vicinity of the resonance energies. These states are calculated by solving the RMF equations with scattering-type boundary conditions for the continuum spectrum. In the RMF-BCS equations the matrix elements of the pairing interaction involving resonant states are calculated by using the scattering states evaluated at the resonance energies and normalized inside a finite region close to the nucleus. The variation of the matrix elements of the pairing interaction due to the widths of the resonant states is taken into account by the derivative of the phase shift. This approximation scheme, used previously in nonrelativistic HF-BCS calculations, is applied here for the neutron-rich Zr isotopes. It is shown that the sudden increase of the neutron radii close to the neutron drip line depends on a few resonant states close to the continuum threshold. Including only these resonant states into the RMF-BCS calculations one gets for the neutron radii and neutron separation energies practically the same results as in the more involved RHB calculations.

ACKNOWLEDGMENTS

We thank J. Meng for useful discussions on RHB calculations. Two of us (N.S. and G.C.H.) acknowledge the financial support from the Japanese Ministry of Education, Science and Technology for research conducted at the RCNP-Osaka. N.S. acknowledges also the support of the Swedish Programme for Cooperation in Research and Higher Education (STINT), and G.C.H. acknowledges the financial support from the National Research Foundation under the Grant No. GUN 2053786.

[1] A. Bohr, B. Mottelson, and D. Pines, Phys. Rev. **110**, 936 (1958).
[2] S. T. Belyaev, A. V. Smirnov, S. V. Tolokonnikov, and S. A. Fayans, Yad. Fiz. **45**, 1263 (1987) [Sov. J. Nucl. Phys. **45**, 783 (1987)].
[3] S. A. Fayans, S. V. Tolokonnikov, and D. Zawischa, Phys. Lett. B **491**, 245 (2000).
[4] A. Bulgac, ICEFIZ- Bucharest; Report No. FT-194-1980; nucl-th/9907088.
[5] M. Grasso, N. Sandulescu, Nguyen Van Giai, and R. J. Liotta, Phys. Rev. C **64**, 064321 (2001).
[6] P. Ring and P. Schuck, *The Nuclear Many-Body Problem* (Springer-Verlag, Berlin, 1980).
[7] P. Ring, Prog. Part. Nucl. Phys. **37**, 193 (1996).
[8] J. Meng and P. Ring, Phys. Rev. Lett. **77**, 3963 (1996).
[9] J. Dobaczewski, H. Flocard, and J. Treiner, Nucl. Phys. **A422**, 103 (1984); J. Dobaczewski *et al.*, Phys. Rev. C **53**, 2809 (1996).
[10] M. Grasso, Nguyen Van Giai, and N. Sandulescu, Phys. Lett. B **535**, 103 (2002).
[11] N. Sandulescu, R. J. Liotta, and R. Wyss, Phys. Lett. B **392**, 6 (1997); N. Sandulescu *et al.*, Phys. Rev. C **61**, 044317 (2000).
[12] N. Sandulescu, Nguyen Van Giai, and R. J. Liotta, Phys. Rev. C **61**, 061301(R) (2000).
[13] M. Del Estal, M. Centelles, X. Vinas, and S. K. Patra, Phys. Rev. C **63**, 044321 (2001).
[14] P. G. Reinhard *et al.*, Z. Phys. A **323**, 13 (1986).
[15] A. B. Migdal, A. M. Perelemov, and V. S. Popov, Yad. Fiz. **14**, 874 (1971) [Sov. J. Nucl. Phys. **14**, 488 (1971)].
[16] H-J. Unger, Nucl. Phys. **A104**, 564 (1967).
[17] J. Meng and P. Ring, Phys. Rev. Lett. **80**, 460 (1998).
[18] M. M. Sharma, M. A. Nagaranjan, and P. Ring, Phys. Lett. B **312**, 377 (1993).
[19] G. A. Lalazissis, J. König, and P. Ring, Phys. Rev. C **55**, 540 (1997).
[20] Y. Sugahara and H. Toki, Nucl. Phys. **A579**, 557 (1994).
[21] G. Audi and A. H. Wapstra, Nucl. Phys. **A595**, 409 (1995).
[22] I. J. Thompson and M. V. Zhukov, Phys. Rev. C **49**, 1904 (1994).